AC6 is the major adenylate cyclase forming a diarrheagenic protein complex with cystic fibrosis transmembrane conductance regulator in cholera

Received for publication, April 9, 2018, and in revised form, May 29, 2018 Published, Papers in Press, June 14, 2018, DOI 10.1074/jbc.RA118.003378

Andrew Thomas[‡1], **Yashaswini Ramananda**[‡§1], **KyuShik Mun**[‡], **Anjaparavanda P. Naren**[‡2], **and Kavisha Arora**[‡3]

From the [‡]*Division of Pulmonary Medicine, Department of Pediatrics, Cincinnati Children's Hospital Medical Center, Cincinnati, Ohio 45229 and the* [§]*Department of Biomedical Sciences, University of Illinois, Chicago, Illinois 60607*

Edited by Roger J. Colbran

The World Health Organization(WHO) has reported a worldwide surge in cases of cholera caused by the intestinal pathogen *Vibrio cholerae*, and, combined, such surges have claimed several million lives, mostly in early childhood. Elevated cAMP production in intestinal epithelial cells challenged with cholera toxin (CTX) results in diarrhea due to chloride transport by a cAMP-activated channel, the cystic fibrosis transmembrane conductance regulator (CFTR). However, the identity of the main cAMP-producing proteins that regulate CFTR in the intestine and may be relevant for secretory diarrhea is unclear. Here, using RNA-Seq to identify the predominant AC isoform in mouse and human cells and extensive biochemical analyses for further characterization, we found that the cAMP-generating enzyme adenylate cyclase 6 (AC6) physically and functionally associates with CFTR at the apical surface of intestinal epithelial cells. We generated epithelium-specific AC6 knockout mice and demonstrated that CFTR-dependent fluid secretion is nearly abolished in AC6 knockout mice upon CTX challenge in ligated ileal loops. Furthermore, loss of AC6 function dramatically impaired CTX-induced CFTR activation in human and mouse intestinal spheroids. Our finding that the CFTR–AC6 protein complex is the key mediator of CTX-associated diarrhea may facilitate development of antidiarrheal agents to manage cholera symptoms and improve outcomes.

Cholera is a disease characterized by severe diarrhea and resultant dehydration, hypovolemic shock, and acidosis (1). Worldwide, 172,454 cholera cases with 1,304 deaths were reported in 2015 to the World Health Organization (WHO).[4] The WHO reports that 41% of these cases were in Africa, 37% in Asia, and 21% in the Americas. More recently, the WHO has reported major outbreaks in Somalia and Yemen with cholera cases currently exceeding one million and growing (http://www.emro.who.int/health-topics/cholera-outbreak/outbreaks.html, accessed April 1st, 2018).[5] It is of significant public health concern that cholera is on an epidemiological rise across the world and continues to claim a significant number of lives, mostly children. Defining precise pathogenic mechanisms of cholera is critical to design preventive and disease control interventions and to prevent such outbreaks.

Cholera is caused by members of the bacterial species *Vibrio cholerae* and is transmitted via a fecal–oral route or consumption of contaminated food and water (1). When virulent cholera bacteria adhere to small bowel, they release cholera enterotoxin (CTX) formed from a B subunit pentamer, for binding to host cells, and an enzymatic A subunit. The endocytosed enzymatic A subunit ADP-ribosylates $G\alpha_s$ subunits of G proteins inside the cell, causing them to remain active. Adenylate cyclases (ACs), the membrane-bound proteins that catalyze the conversion of ATP to cAMP and pyrophosphate, are, in general, activated via $G\alpha_s$ pathways (2). Hence, at a molecular level, CTX challenge translates into excessive cAMP production by ACs and activation of cAMP-dependent protein kinase A (PKA). Severe diarrhea in cholera occurs due to PKA-mediated phosphorylation and then hyperactivation of cystic fibrosis transmembrane conductance regulator (CFTR) protein, which continues to electrochemically drive water into the intestinal lumen coupled to its chloride transport activity (3). CFTR is a key member of the secretory epithelium in the gut and the lung that regulates overall fluid transit by means of its chloride transport function (4). Loss of CFTR function results in cystic fibrosis (CF), a fatal disease that affects multiple organs (5). The most common cause of CF is the Phe-508 deletion (F508del) mutation in CFTR that generates a clinically significant processing

This work was supported by National Institutes of Health Grants DK080834 and DK093045 (to A. P. N.) and Cystic Fibrosis Foundation Grants ARORA16F0 (to K. A.) and NAREN 14XX0 (to A. P. N.). The authors declare that they have no conflicts of interest with the contents of this article. The content is solely the responsibility of the authors and does not necessarily represent the official views of the National Institutes of Health.
This article was selected as one of our Editors' Picks.

[1] Both authors contributed equally to this work.
[2] To whom correspondence may be addressed: Division of Pulmonary Medicine, Dept. of Pediatrics, 3333 Burnet Ave. MLC 2021, Cincinnati Children's Hospital Medical Center, Cincinnati, OH 45229. Tel.: 513-803-4731; Fax: 513-803-4783; E-mail: anaren@cchmc.org.
[3] To whom correspondence may be addressed: Division of Pulmonary Medicine, Dept. of Pediatrics, 3333 Burnet Ave. MLC 2021, Cincinnati Children's Hospital Medical Center, Cincinnati, OH 45229. Tel.: 513-803-7628; Fax: 513-803-4783; E-mail: kavisha.arora@cchmc.org.

[4] The abbreviations used are: WHO, World Health Organization; CTX, cholera toxin; AC, adenylate cyclase; PKA, protein kinase A; CF, cystic fibrosis; CFTR, cystic fibrosis transmembrane conductance regulator; F508del, Phe-508 deletion; Shh, sonic hedgehog; R, regulatory; PLA, proximity ligation assay; aa, amino acids; FSK, forskolin; ANOVA, analysis of variance; CPT-cAMP, chlorophenylthio-cAMP; FRETc, corrected FRET; N-FRETc, normalized corrected FRET.
[5] Please note that the JBC is not responsible for the long-term archiving and maintenance of this site or any other third party hosted site.

defect in the protein and little to no function of CFTR at the plasma membrane. CFTR has been established as the primary driver of CTX-induced diarrhea based on studies in CF mice (6). CFTR can be regulated by multiprotein complex formation consisting of protein kinases, scaffolding proteins, ion channels, cytoskeletal elements, and other transporters (7, 8). Protein–protein interactions of CFTR have been shown to play important roles in CFTR trafficking, channel regulation, compartmentalized signaling to optimize CFTR function, and surface stabilization (7–10).

There are currently nine membrane-bound AC isoforms (*Adcy1–9*) identified in mammalian cells (11). The predominant AC isoform that regulates CFTR in the intestine and is relevant to secretory diarrhea has not been clearly determined (12). In this study, we elucidated that CFTR and AC6 signaling complex formation is responsible for CTX-induced diarrhea and that loss of AC6 in mice is protective against diarrhea. Our findings identify the primary diarrheagenic protein complex in cholera, presenting an opportunity to develop specific anti-diarrheal agents targeted at these complexes.

Results

AC6 is the most abundant AC isoform in the gut

Cellular cAMP generation is determined by the relative expression and distribution of different ACs. To determine the relative expression of ACs in gut epithelial cells, we used mRNA sequencing in mouse and human intestinal epithelial cells. We found AC6 to be the predominant AC isoform in these cells (Fig. 1*A*), which led us to further investigate the role of AC6 in intestinal physiology and pathophysiology. We generated an epithelium-specific knockout of AC6 using a sonic hedgehog cre recombinase (Shh Cre) driver and confirmed loss of AC6 protein expression in $Adcy6^{f/f\ Shh\ Cre/+}$ ($Adcy6^{\Delta/\Delta}$) mouse ileum (Fig. 1, *B–E*). Immunostaining data revealed apical enrichment of AC6 in the mouse ileum (Fig. 1*E*). CFTR is an apical membrane-localized chloride channel in the gut and airway epithelial cells (8). CFTR is composed of two membrane-spanning domains, two nucleotide-binding domains, and a unique intracellular regulatory (R) domain of ~240 amino acids (residues 590–830) (13). CFTR is activated by PKA-mediated phosphorylation of serine residues in the R domain and binding and hydrolysis of intracellular ATP at the nucleotide-binding domains. Phosphorylation of the R domain is required for opening of the CFTR channel. Based on these earlier reported data and our findings, we tested how cAMP generation by apical AC6 may regulate CFTR function.

AC6 interacts directly with CFTR in intestinal epithelial cells

Based on an exclusive apical localization of CFTR and AC6 in the gut epithelial cells, we considered the possibility that CFTR and AC6 might interact with each other. In a co-immunoprecipitation assay, we detected AC6 in complex with CFTR in the isolated $Adcy6^{f/f}$ intestinal mucosa, whereas the band corresponding to AC6 was negligibly detected in $Adcy6^{\Delta/\Delta}$ mucosa (Fig. 2*A*). Importantly, in this experiment, we observed that loss of AC6 did not impact CFTR protein expression (Fig. 2*A*). We determined, using a FRET assay, that AC6 and CFTR interact at the plasma membrane in live colon epithelial cells (HT29CL19a) (Fig. 2, *B* and *C*). In addition, we performed proximity ligation assays (PLAs) to detect *in situ* AC6–CFTR interactions in mouse and human intestinal epithelial cells. PLA is a highly sensitive and specific immunoassay-based technology that has been designed to quantitate proteins and detect protein interactions and modifications within a spatial span of 40 nM (14). Using this method, we detected positive PLA signal corresponding to CFTR–AC6 complex at the apical membrane in $Adcy6^{f/f}$ intestinal epithelial cells (Fig. 2, *D* and *E*). A PLA signal was present in negligible quantities in $Adcy6^{\Delta/\Delta}$ intestine (Fig. 2, *D* and *E*). Similarly, we found a positive PLA signal corresponding to CFTR–AC6 interaction in human intestinal spheroids that was enriched at the apical or luminal side (Fig. 2*F*). To identify which cytosolic regions of AC6 may interact with CFTR, we generated His-S–tagged cytosolic domains of AC6 (C1 (306–672 aa) and C2 (917–1165 aa)), which together constitute the catalytic core of AC6 protein, and expressed these constructs in a bacterial protein expression system. Using S-protein pulldown, we detected an interaction of FLAG-CFTR with AC6 C2 (Fig. 2*G*). The interaction of AC6 C2 was maintained with FLAG-$CFTR_{His10}$, suggesting that the interaction does not require the canonical C-terminal PDZ motif in CFTR (Fig. 2*G*). Overall, we determined that AC6 forms a protein complex with CFTR, and, given the high abundance of the AC6 protein in intestinal epithelial cells, we hypothesized that this protein complex may potentially become the major physiological driver of CFTR function.

cAMP generation is attenuated in $Adcy6^{\Delta/\Delta}$ intestinal epithelial cells

Based on the abundance of AC6 in intestinal epithelial cells, we investigated how loss of AC6 affects intracellular cAMP levels. We isolated intestinal crypts from $Adcy6^{f/f}$ and $Adcy6^{\Delta/\Delta}$ ileum and cultured them in a Matrigel-based matrix. Subsequently, we measured cAMP levels using ELISA and detected dramatically reduced cAMP production in $Adcy6^{\Delta/\Delta}$ compared with $Adcy6^{f/f}$ intestinal epithelial cells in response to the AC agonist forskolin (FSK) (Fig. 3*A*). In addition, the CTX-induced increase in intracellular cAMP levels was significantly diminished in $Adcy6^{\Delta/\Delta}$ intestinal epithelial cells (Fig. 3*B*). Production of intracellular cGMP upon guanylate cyclase activation by linaclotide (15), a peptide analog of heat-stable enterotoxin, did not differ between $Adcy6^{f/f}$ and $Adcy6^{\Delta/\Delta}$ intestinal epithelial cells (Fig. 3*C*). Because CTX failed to produce diarrhea-inducing flux of intracellular cAMP in $Adcy6^{\Delta/\Delta}$ cells, we proceeded to investigate how loss of AC6 affects CFTR function upon CTX challenge.

$Adcy6^{\Delta/\Delta}$ mice are protected against CTX-induced diarrhea

Having determined that AC6 and CFTR interact at the plasma membrane and that loss of AC6 fails to elicit cAMP response in the presence of CTX, we next investigated intestinal fluid secretion in $Adcy6^{\Delta/\Delta}$ mice upon CTX challenge. We used the closed ileal loop model in mice to test CTX-induced fluid secretion (3, 6, 16, 17). CTX injected into the ligated loops induces hyperactivation of CFTR Cl^- channel via cAMP production, causing a voluminous fluid secretion and accumulation in the closed loops. Consistently, chemical inhibition of CFTR function (*e.g.* using CFTRinh-172) or loss-of-function

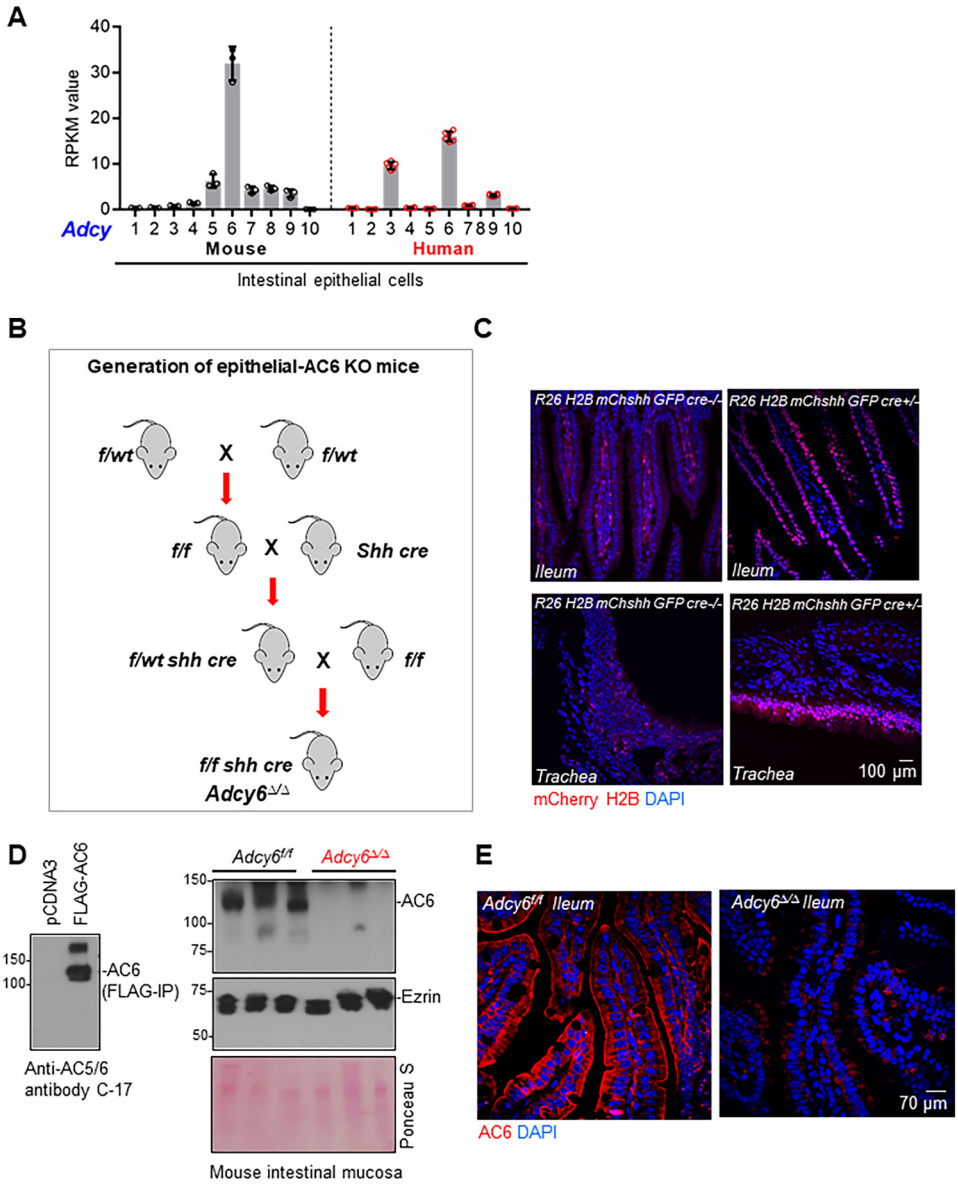

Figure 1. AC6 is the most dominant AC isoform in the gut. *A*, RNA-Seq data demonstrate relative abundance of ACs in the mouse ($n = 3$) and human intestinal epithelial cells ($n = 6$). *Error bars*, S.D. *B*, breeding scheme followed to generate *Adcy6*$^{\Delta/\Delta}$ (*Adcy6*$^{flox/flox}$ *shhCre*$^{+}$) mice. *C*, confocal images demonstrate Cre recombinase activity detected in small intestine and trachea using R26 H2B mCh Cre reporter. *f*, floxed allele; *wt*, WT allele; *shh*, sonic hedgehog; *cre*, Cre recombinase; *R26 H2B mChshh*, Rosa26 histone 2B mcherry shh reporter. *Red signal* corresponding to histone 2B mcherry indicates positive Cre expression. *D*, Western blotting data (*left*) show that AC5/6 antibody (see "Materials and methods") used in the study recognizes purified FLAG-tagged AC6 (immunoprecipitated using FLAG beads from HEK 293 FLAG-AC6 stable cell line). *Right*, AC6 expression in membrane fraction prepared from *Adcy6*$^{f/f}$ and *Adcy6*$^{\Delta/\Delta}$ mouse ileum and probed using AC5/6 antibody. Ezrin was used as a loading control. *E*, immunostaining data corresponding to AC5/6 expression (*red*) detected using AC5/AC6 antibody in ileum sections isolated from *Adcy6*$^{f/f}$ and *Adcy6*$^{\Delta/\Delta}$ mice. Nuclei were counterstained with DAPI (*blue*).

mutation in CFTR (*e.g.* F508del CFTR) makes CTX less effective or ineffective in inducing secretion in ligated ileal loops in mice (16, 17). Whereas CTX induced significant fluid accumulation in *Adcy6*$^{f/f}$ mice, this phenomenon was largely absent in *Adcy6*$^{\Delta/\Delta}$ mice at a CTX dose of 1 μg and dramatically impaired at a dose of 10 μg (Fig. 4, *A* and *B*). Importantly, cGMP-induced fluid secretion in the ileal loops in response to linaclotide was not significantly different between *Adcy6*$^{f/f}$ and *Adcy6*$^{\Delta/\Delta}$ mice (Fig. 4, *A* and *B*). These findings support the conclusion that AC6 is required for CTX-induced diarrhea. Also, loss of AC6 does not impair the functional ability of cAMP-independent activation of CFTR (*e.g.* by cGMP in intestinal epithelial cells). To determine the effect of loss of AC6 on CFTR chloride channel function, we measured cAMP-stimulated short-circuit currents. CFTR-dependent Cl^- currents were monitored in tracheal epithelial cells isolated from *Adcy6*$^{f/f}$ and *Adcy6*$^{\Delta/\Delta}$ mice and polarized on the transwells. As the *shh cre* driver is highly expressed in tracheal epithelial cells in addition to intestinal cells (Fig. 1*C*) and we confirmed loss of AC6 in the tracheal epithelial cells (Fig. 4*C*), it was appropriate to test tracheal epithelial cells to monitor CFTR-mediated Cl^- transport as a function of loss of AC6. CFTR-dependent Cl^- currents were reduced by 3.2-fold in *Adcy6*$^{f/f}$ *versus Adcy6*$^{\Delta/\Delta}$ mice (Fig. 4, *D* and *E*). Purinergic receptor stimulation by ATP that elicits calcium-dependent Cl^- currents generated a similar response in *Adcy6*$^{f/f}$ and *Adcy6*$^{\Delta/\Delta}$ tracheal cells (Fig. 4, *D* and *E*). Hence, AC6 is the primary AC to

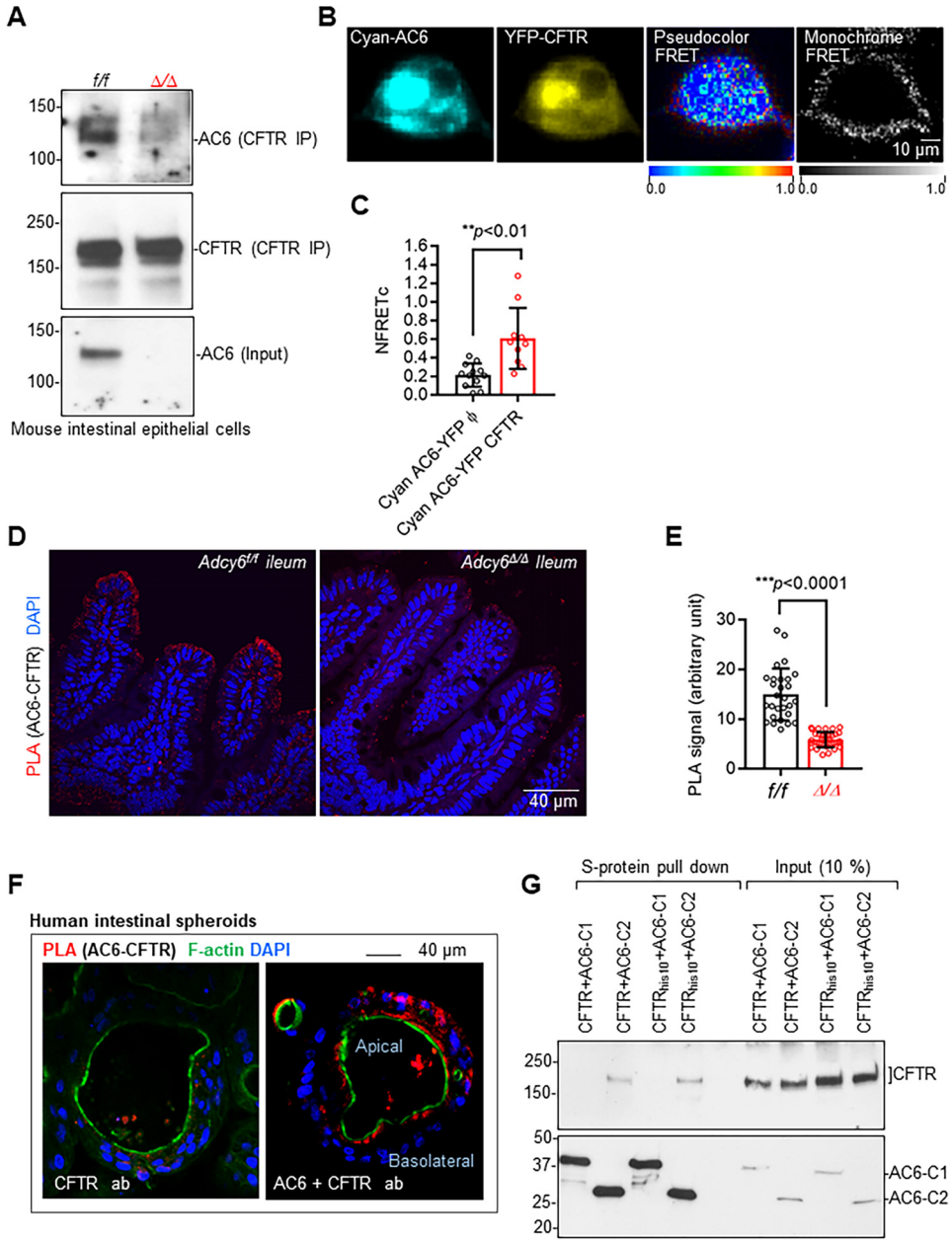

Figure 2. AC6 interacts directly with CFTR. *A*, Western blotting data show co-immunoprecipitation of CFTR from *Adcy6*$^{f/f}$ and *Adcy6*$^{\Delta/\Delta}$ mouse intestinal epithelial cells detecting AC6 in complex with CFTR. CFTR was immunoprecipitated (*IP*) from Matrigel-embedded *Adcy6*$^{f/f}$ and *Adcy6*$^{\Delta/\Delta}$ murine intestinal epithelial cells, using protein A/G–cross-linked M3A7 CFTR antibody. The Western blotting was probed using AC5/6 antibody. This experiment was repeated twice and generated similar data. *B*, sensitized FRET or NFRETc data marked by *pseudocolor* and *monochrome images* in HT29CL19A cells depict an interaction between Cyan-AC6 (FRET donor) and yellow fluorescent protein–CFTR (FRET acceptor) at the plasma membrane. *C*, quantitation of NFRETc value (equivalent to FRET efficiency) from $n = 3$ independent experiments as represented in *B*. *Error bars*, S.D. *p* value was determined by *t* test. *D*, confocal images demonstrate PLA signal (*red*) corresponding to an interaction between CFTR and AC6 in *Adcy6*$^{f/f}$ and *Adcy6*$^{\Delta/\Delta}$ mouse ileum. PLA signal was dramatically reduced in *Adcy6*$^{\Delta/\Delta}$ mouse ileum. *E*, quantitation of PLA signal in *Adcy6*$^{f/f}$ and *Adcy6*$^{\Delta/\Delta}$ mouse ileum as represented in *D* from $n = 3$ independent experiments. *Error bars*, S.D. *p* value was determined by *t* test. *F*, confocal images demonstrate PLA signal (*red*) corresponding to an interaction between CFTR and AC6 in human intestinal epithelial cells (*right*). Only CFTR antibody was added, and the PLA was performed for a negative control (*left*). This experiment was repeated two times and generated similar data. *G*, Western blotting data shows interaction of His-S–AC6 C2 (917–1165 aa) domain but not His-S–AC6 C1 (306–672 aa) with FLAG-CFTR and FLAG-CFTR$_{His10}$ immunoprecipitated from whole-cell lysate from BHK cells stably expressing CFTR proteins using S-protein–conjugated resin. To detect CFTR protein, Western blotting was probed using FLAG-CFTR antibody. His-S–tagged AC6 C1 (306–672 aa) and AC6 C2 (917–1165 aa) proteins were detected using S-HRP antibody. This experiment was repeated up to seven times and generated similar data.

mediate cAMP-dependent activation of CFTR that drives diarrhea in cholera and CFTR activation in the large airways.

Loss of AC6 impairs fluid secretion in human- and mouse-derived enterospheres

Intestinal organoids/enterospheres are cultured three-dimensional epithelial structures that contain the key intestinal cell types and recapitulate the functional features of the native intestinal tissue (18, 19). Enterosphere-based fluid secretion assay is a method that can specifically determine CFTR function (9, 20). Because of high expression of CFTR in the enterospheres, CFTR activation using forskolin causes rapid luminal area expansion that can be quantitated (9, 20). Luminal expansion is perturbed upon chemical inhibition of CFTR function

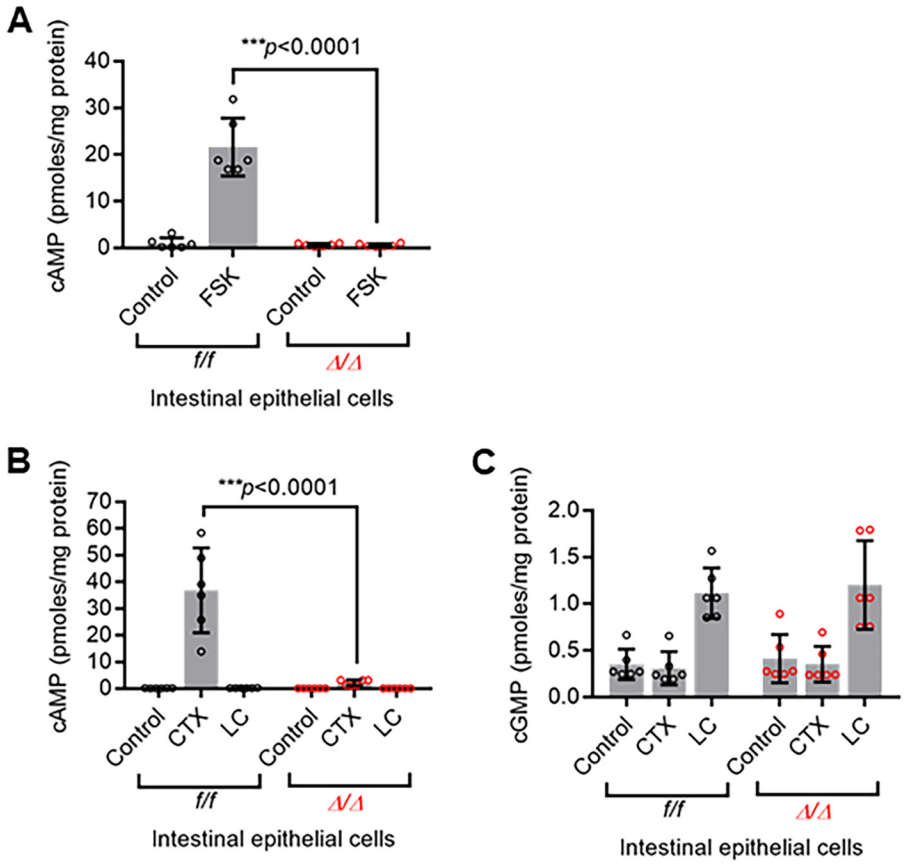

Figure 3. cAMP generation is impaired in *Adcy6*$^{\Delta/\Delta}$ intestinal epithelial cells. *Bar graphs* represent whole-cell cAMP measurement in response to FSK (10 μM, 1 h) (*A*) and CTX (100 ng, 24 h) and linaclotide (*LC*; 500 ng, 24 h) (*B*) and whole-cell cGMP measurement in response to CTX (100 ng, 24 h) and linaclotide (500 ng, 24 h) (*C*) (same samples as used in *B*) in intestinal epithelial cells derived from *Adcy6*$^{f/f}$ and *Adcy6*$^{\Delta/\Delta}$ mice. Each *dot* represents a single measurement from an $n = 3$ intestinal cell preparation. *Error bars*, S.D. *p* value was determined by ANOVA with Bonferroni's multiple-comparison test.

(*e.g.* using CFTRinh-172), loss of CFTR (*e.g.* due to premature termination codon in CFTR), and loss-of-function mutations in CFTR (*e.g.* F508del CFTR) (9, 20). Enterospheres are valuable models to study the effect of physiological modulators (*e.g.* cAMP signaling) on CFTR function. Therefore, we assessed luminal expansion of day 3 enterospheres derived from *Adcy6*$^{f/f}$ and *Adcy6*$^{\Delta/\Delta}$ mice in response to cAMP agonists. Whereas *Adcy6*$^{f/f}$ enterospheres demonstrated robust luminal expansion in response to FSK in a dose-dependent manner, this response was severely impaired in *Adcy6*$^{\Delta/\Delta}$ enterospheres (Fig. 5, *A* and *B*). We knocked down AC6 expression in human enterospheres (day 7) using two cycles of transduction with AC6 lentiviral shRNA and observed obliterated luminal expansion in enterospheres in response to FSK (Fig. 5*C*). CTX-induced luminal expansion was negligible in *Adcy6*$^{\Delta/\Delta}$ day 3 enterospheres relative to *Adcy6*$^{f/f}$ enterospheres (Fig. 5*D*). However, the cell-permeant CPT-cAMP analog that works independently of AC activity and robustly activates CFTR and the cGMP agonist linaclotide generated similar luminal expansion in both *Adcy6*$^{\Delta/\Delta}$ and *Adcy6*$^{f/f}$ enterospheres (Fig. 5*E*). This finding suggests that *Adcy6*$^{\Delta/\Delta}$ enterospheres are functionally viable in terms of CFTR function but are just not responsive to AC agonist FSK. Hence, AC6 is the principle cAMP source for CFTR activation in enterospheres. We measured CFTR-mediated fluid secretion in the enterospheres in a time-dependent manner using a high-content microscope and observed less fluid secretion (measured by expansion of the enterosphere area) in *Adcy6*$^{\Delta/\Delta}$ enterospheres compared with *Adcy6*$^{f/f}$ enterospheres (Fig. 6, *A* and *B*). Overall, loss of AC6 reduces the magnitude of CFTR-dependent fluid secretion in the enterospheres.

Discussion

CFTR is an important channel that controls one of the key functions of the intestinal epithelium (*i.e.* fluid homeostasis). Excessive activation of CFTR causes secretory diarrhea, whereas loss of CFTR function may lead to chronic constipation or to meconium ileus in some CF cases. Both of these scenarios are serious health issues.

Our results collectively demonstrate that AC6–CFTR macromolecular complex formation principally drives CFTR-dependent hypersecretion upon CTX challenge. Our findings present an avenue for development of novel anti-diarrheal agents to treat cholera that currently poses a massive health threat in many parts of the world. Small molecules that could specifically inhibit AC6 activity may prove beneficial to control cholera. Whereas administering osmolytes is the cheapest and simplest approach to prevent and treat dehydration in cholera to avert fatality, this does not control diarrhea, address the root cause of cholera, or mitigate the pathogenic effects of chronic cAMP production during cholera. Balancing cellular cAMP is necessary, as excessive cAMP can ectopically influence multiple signaling pathways and may even lead to cell toxicity (21).

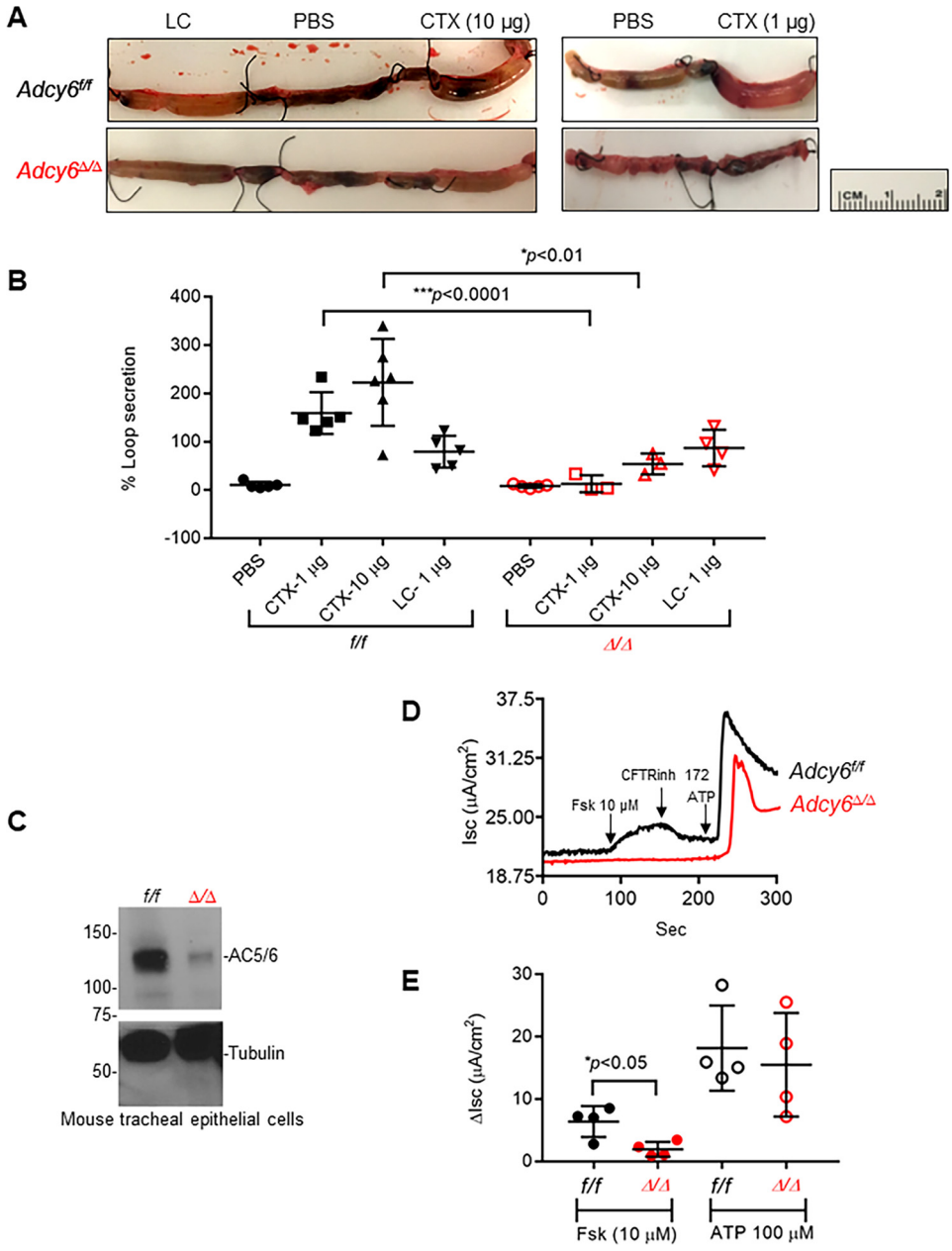

Figure 4. *Adcy6*$^{\Delta/\Delta}$ mice are protected against CTX-induced diarrhea. *A*, representative images of distal intestinal loops from the small intestine of *Adcy6*$^{f/f}$ and *Adcy6*$^{\Delta/\Delta}$ mice injected with PBS, CTX (1 and 10 μg), and linaclotide (*LC*; 1 μg) for 6 h to stimulate CFTR function. A *scale bar* is shown on the *right*. *B*, *dot plot* shows measurement of the net fluid secretion in the intestinal loops collected at 6 h post-surgery to measure fluid secretion in response to PBS, CTX, and linaclotide. Each *dot* represents a single loop. *C*, Western blotting depicts expression of AC6 in *Adcy6*$^{f/f}$ and *Adcy6*$^{\Delta/\Delta}$ mouse tracheal epithelial cells probed using AC5/6 antibody. Tubulin was used as a loading control. *D*, representative traces of short-circuit currents (I_{sc}) in polarized *Adcy6*$^{f/f}$ and *Adcy6*$^{\Delta/\Delta}$ tracheal epithelial cells. Currents were stimulated in the presence of apical FSK (10 μM) followed by the addition of CFTRihn-172 (10 μM) on the apical side. At the end of the experiment, calcium-dependent Cl^- currents were stimulated in the presence of ATP (100 μM) on the apical side. *E*, *dot plot* shows change in I_{sc} (ΔI_{sc}) measurement in the presence of the indicated treatments from the I_{sc} traces as represented in *C*. Each *dot* corresponds to a single I_{sc} trace. *Error bars*, S.D. in all of the quantitative data above. *p* value was determined by ANOVA with Bonferroni's multiple-comparison test.

This is particularly important because AC6 is such an abundant protein in the intestinal epithelial cells. Based on our data, regulation of AC6 through a small-molecule inhibitor is theoretically one of the most effective ways to control cholera. The use of a highly specific CFTR inhibitor (CFTRinh-172) as an antidiarrheal agent could not be successful because of associative toxicity of the compound (22). Therefore, we need to not only develop safer anti-diarrheal drugs but also identify multiple targets in cholera that can be targeted with minimal side effects. Studies elucidating the roles of ACs in human diseases have been limited by the lack of specific reagents for ACs (inhibitors, activators, and antibodies) (23). We sufficiently validated that the AC5/6 antibody used in the study recognizes AC6. Many times, we resorted to using recombinant AC6 (with FLAG or fluorescent tag) for the sole purpose of validation. We also hope that defining these AC-specific roles in human diseases will incentivize related product development within pharmaceutical industries.

The relatively high abundance of AC6 in the intestine and its close proximity to CFTR through a direct interaction indicate

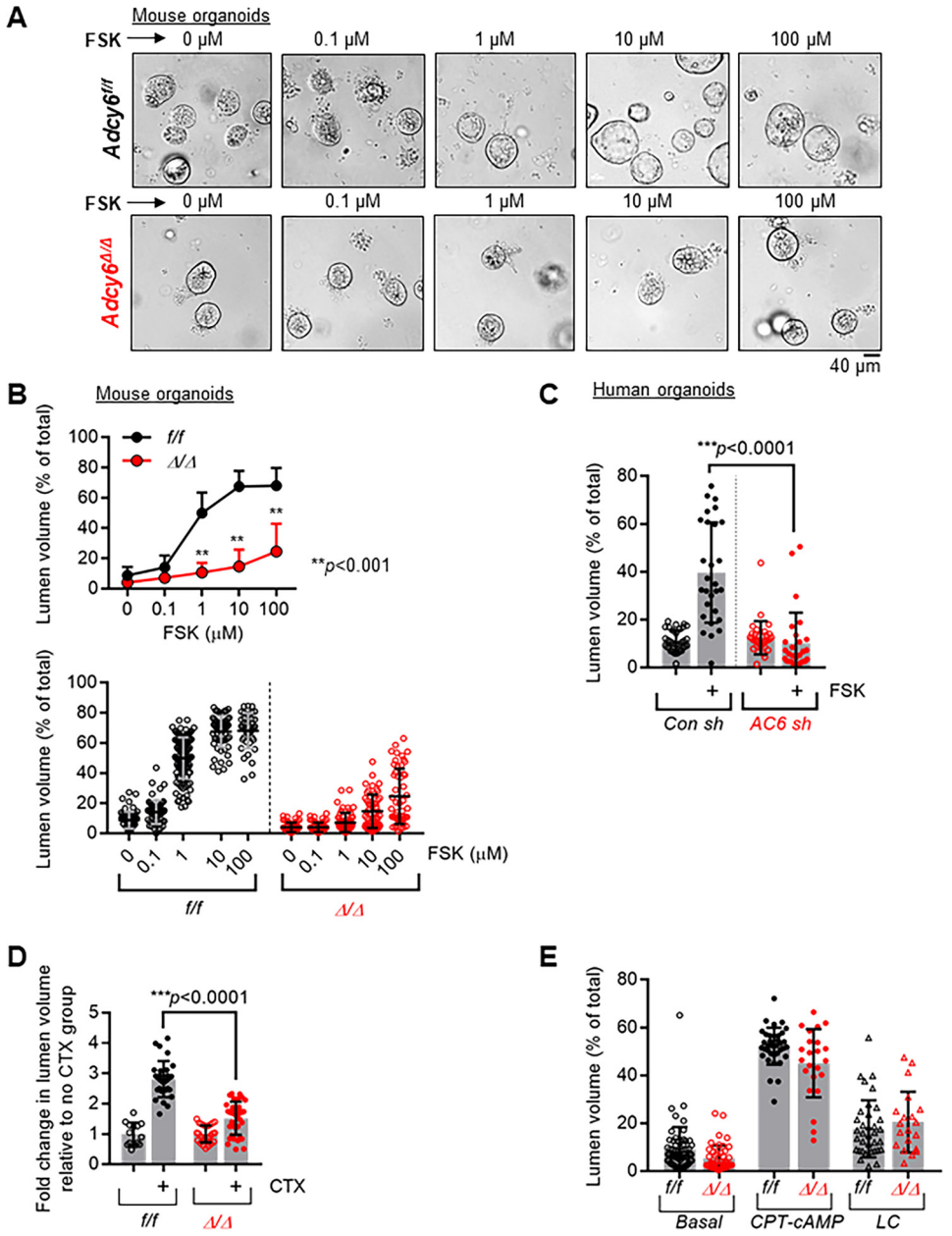

Figure 5. *Adcy6*$^{\Delta/\Delta}$ mouse–derived enterospheres show impaired cAMP-induced fluid secretion. *A*, representative images of *Adcy6*$^{f/f}$ and *Adcy6*$^{\Delta/\Delta}$ enterospheres depict fluid secretion under increasing dose of FSK (0–10 μM) and monitored for 30 min. *B*, *top*, *line graph* represents quantitation of fluid secretion as represented in *A*. *Bottom*, *dot plot* depicts individual data points corresponding to fluid secretion in enterospheres as represented in *A*. This experiment was averaged from enterospheres derived from $n = 3$ mice. *C*, quantitation of fluid secretion with or without FSK (10 μM) in human-derived enterospheres pretreated with control and AC6 shRNA lentiviral particles. This experiment was averaged from enterospheres from $n = 3$ independent experiments from a single human donor. Each *dot* represents a single enterosphere. *D*, quantitation of fluid secretion with or without CTX (1 μg/ml) in *Adcy6*$^{f/f}$ and *Adcy6*$^{\Delta/\Delta}$ enterospheres monitored after 24-h treatment and represented as -fold change relative to no CTX group. This experiment was averaged from enterospheres from $n = 3$ mice. Each *dot* represents a single enterosphere. *E*, *bar graph* depicts fluid secretion with or without CPT-cAMP (100 μM) and linaclotide (*LC*; 500 nM) in *Adcy6*$^{f/f}$ and *Adcy6*$^{\Delta/\Delta}$ enterospheres monitored after 2-h treatment. This experiment was averaged from enterospheres from $n = 3$ mice. Each *dot* represents a single enterosphere. *Error bars*, S.D. in all of the quantitative data above. *p* value was determined by ANOVA with Bonferroni's multiple-comparison test.

why CTX-induced diarrhea becomes so exaggerated. The minimal CTX-generated fluid secretion response in *Adcy6*$^{\Delta/\Delta}$ mice suggests that other ACs may not be able to compensate for the loss of AC6 in terms of CFTR activation and formation of cellular cAMP upon CTX challenge. Only at high doses of FSK (100 μM) and CTX (10 μg) were AC6-independent mechanisms of stimulation of fluid secretion evident. We anticipate that the global cAMP generation by other ACs would stimulate CFTR-dependent fluid secretion at high doses of cAMP agonists in AC6 knockout mice; however, the fluid secretion stayed dramatically poor relative to the WT mice. There are several lines of experimental evidence to support that cAMP signaling operates in a largely compartmentalized fashion, which enables more specificity and faster kinetics of the signaling processes, underscoring the importance of cAMP compartmentalization in normal cell physiology (23, 24). Each AC isoform, although producing a common signaling molecule, cAMP, is subject to differential regulation by signaling processes (23, 25). There-

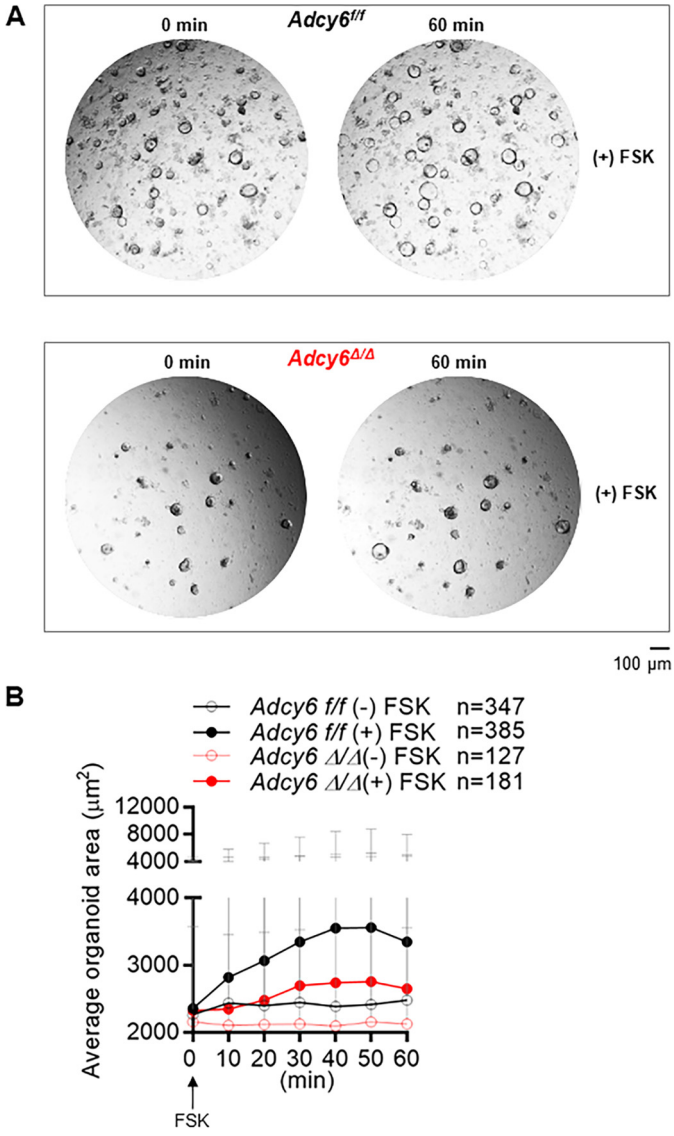

Figure 6. *Adcy6*$^{\Delta/\Delta}$ mouse–derived enterospheres show reduced fluid secretion in a high-content assay. *A*, representative images of *Adcy6*$^{f/f}$ and *Adcy6*$^{\Delta/\Delta}$ enterospheres taken in a high-content automated microscope depict fluid secretion in response to FSK (10 μM) added at 0 min and followed up to 60 min. (−) FSK groups represent enterospheres without any FSK treatment. *B*, *line graph* depicts time-dependent measurement of average area of *Adcy6*$^{f/f}$ and *Adcy6*$^{\Delta/\Delta}$ enterospheres monitored in a high-content automated microscope following treatment with FSK (10 μM) at 0 h for (+) FSK samples. The total number of enterospheres tested in the experiment are shown in the graph legend. *Error bars*, S.D.

fore, not all AC isoforms perform indistinguishable functions. Localization in different cellular compartments and association with specific G protein–coupled receptors and other downstream effector proteins provide means of cAMP signaling compartmentalization. Formation of macromolecular protein complexes, as in this study, between CFTR and AC6 is an elegant example of compartmentalized cAMP signaling enabling a higher degree of specificity toward CFTR activation.

It is argued that Na^+ absorption may contribute to fluid accumulation in the enteroids at high doses of cAMP agonists, as NHE3-dependent pH activity has been detected in the enteroids (26). In the undifferentiated or proliferative state (as were the intestinal organoids used in this study), Na^+ absorption causes minimal luminal expansion in response to FSK over a short time period (30 min). Fluid secretion in response to FSK is completely absent in F508del/F508del *cftr* mouse enteroids measured within 2 h of stimulant addition as previously demonstrated by us (9). This suggests that in an acute assay, fluid secretion in the enterospheres is largely CFTR-mediated. As a result, we kept the window of measurement of secretion in the enterospheres ≤2 h. On an important note, loss of AC6 did not inhibit the process of organoid formation and closure, and CFTR expression was not affected in *Adcy6*$^{\Delta/\Delta}$ enterospheres.

Our study demonstrates that AC6 is an important modifier of CFTR function. We find these studies not only relevant to cholera toxin–induced diarrhea but to CF as well. There are data suggesting that the most common CF mutation, F508del CFTR, shows diminished phosphorylation by PKA (27, 28). This effect correlated with the altered channel activity and kinetics of activation of the mutant protein at the plasma membrane. These properties of F508del CFTR are very much reflective of the way AC6 regulates normal CFTR. It would be interesting to investigate whether there is a perturbed interaction of the mutant CFTR protein with AC6. Previously, we demonstrated that F508del CFTR behaves poorly in terms of PDZ-dependent interactions compared with normal CFTR, which translates into reduced half-life and function of the rescued mutant protein at the plasma membrane (9). Understanding how peripheral interactions are orchestrated and regulate CFTR behavior is critical to determine the functional efficiency of rescued F508del CFTR. Also, it will be important to determine how the most stimulatory interactions, one of which according to our data is CFTR–AC6, can be selectively enhanced to benefit F508del CFTR function in combination with other approaches.

Materials and methods

Statistics

The statistical significance was calculated using Student's *t* test or one-way ANOVA with multiple-comparison tests as applicable. $p < 0.05$ was considered statistically significant.

Chemicals and antibodies

Chemicals used in this study include forskolin, CPT-cAMP, isobutylmethylxanthine, and CTX from MilliporeSigma. Antibodies in this study included anti-CFTR M3A7 (Thermo Fisher Scientific) and CF3 (Abcam, Cambridge, UK), anti-AC5/6 (Santa Cruz Biotechnology, Dallas, TX), and anti-ezrin and tubulin (Cell Signaling Technologies, Danvers, MA). Linaclotide was provided by Ironwood Pharmaceuticals for research application. Ready-to-transduce GIPZ lentiviral shRNA particles (human scrambled and AC6 shRNAs) were obtained from GE Dharmacon. For lentiviral knockdown, human enterospheres were treated with the viral particles (1×10^5 transducing units) for 48 h followed by 48 h of recovery and then again treated for 48 h before the experiment.

Mice

Adcy6$^{f/wt}$ mice (Jackson Laboratory) were interbred to obtain *Adcy6*$^{f/f}$ mice. *Adcy6*$^{f/f}$ female mice were crossed with male Shh

GFP Cre mice (B6.Cg-*Shh*$^{tm1(EGFP/cre)Cjt/J}$, Jackson Laboratory) to finally obtain *Adcy6*$^{\Delta/\Delta}$ mice (*Adcy6*$^{f/f}$ *Shh*$^{tm1(EGFP/cre)/wt}$ mice). Typically, 6–12-week-old male mice were used for the study. All of the mice were maintained in a barrier facility at Cincinnati Children's Hospital Medical Center and were fed normal chow. All procedures were performed in compliance with the Association for Assessment and Accreditation of Laboratory Animal Care and institutional guidelines and were approved by the Cincinnati Children's Hospital Medical Center institutional animal care and use committee.

Human biopsy tissues

Retrieval of patient biopsies for research use was approved by the Cincinnati Children's Hospital Medical Center institutional review board under IRB 2014-6279.

Cell lysate preparation, protein purification, and protein-binding assays

Crude membrane preparation of Adcy6$^{f/f}$ *and Adcy6*$^{\Delta/\Delta}$ *mouse ileum*—Small intestinal mucosa was cut into small pieces and transferred to a Dounce homogenizer. Next, 1–2 ml of cold homogenization buffer (250 mM sucrose, 1 mM EDTA, 10 mM Tris HCl buffer, pH 7.2) plus protease inhibitors (1 μM aprotinin, 1 μM leupeptin, and 1 mM phenylmethylsulfonyl fluoride) was added to the homogenizer. Tissue was homogenized using ~20 manual up and down strokes a total of three times. Samples were transferred to microcentrifuge tubes. Intact cells, nuclei, and cell debris were removed by centrifugation of the homogenate at 500 × *g* for 10 min at 4 °C. The supernatant was the postnuclear supernatant. The postnuclear supernatant was centrifuged at 145,000 × *g* for 1 h at 4 °C. The supernatant following the centrifugation contained soluble proteins (cytosolic fraction). The pellet comprised the crude membrane fraction and was washed with homogenization buffer twice. The glass tube was sonicated for 20 s three times at 30-s intervals to dissolve the pellet. Protein concentration was measured using a Bradford assay, and samples were protein normalized before loading for running Western blotting.

Adcy6$^{f/f}$ and *Adcy6*$^{\Delta/\Delta}$ intestinal epithelial cells were lysed in PBS plus 0.2% Triton X-100-containing protease inhibitor cocktail. CFTR was immunoprecipitated from whole-cell lysates by cross-linking M3A7 CFTR antibody to protein A–agarose (0.5 μg of antibody per 10 μl of protein A–conjugated resin by using disuccinimidyl suberate crosslinker). Proteins immobilized on beads were eluted using glycine-based elution buffer (pH 2) containing 0.2% Triton X-100. Samples were incubated for 10 min at 37 °C and subjected to SDS-PAGE and Western blotting. FLAG-AC6 was immunoprecipitated from FLAG-AC6 HEK 293 stable cell line using FLAG-conjugated resin (MilliporeSigma) and eluted using low-pH glycine buffer as described above.

Purification of His-S–tagged AC6 C1 (306–672 aa) and AC6 C2 (917–1165 aa) domains—AC6 C1 (306–672 aa) and AC6 C2 (917–1165 aa) cDNAs were inserted into pTriEx4 (Novagen) expression constructs followed by transformation into Origami competent cells. Bacteria transformed with the constructs were lysed in resuspension buffer containing 25 mM HEPES-KOH, 400 mM KCl, and 5 mM β-mercaptoethanol (added fresh), followed by adding lysozyme (1 mg/ml) prepared in resuspension buffer for 30 min at 4 °C. Next, 2.1% Triton X-100 was added to the lysate and mixed for another 30 min at 4 °C. Lysate was transferred to clean centrifuge tubes and centrifuged at 10,000 × *g* for 30 min at 4 °C. To the clear supernatant, 100 μl of TALON® beads (Clontech) were added and mixed for 2–3 h at 4 °C. TALON® beads containing proteins were washed 3–4 times with PBS plus 0.2% Triton X-100 and resuspension buffer, respectively, in the presence of protease inhibitors. His-tagged proteins were eluted with 200 mM imidazole, 1–4 times. Protein concentrations of the samples were quantified by using a Bradford assay or by direct absorbance at 280 nm. To perform the binding assay between AC6 C1/C2 and CFTR, 50 μg of the C1/C2 protein was added to 1 mg of protein from whole-cell BHK lysate expressing FLAG-CFTR or FLAG-CFTR$_{His10}$. Protein complexes were immunoprecipitated using S-protein–conjugated agarose in an overnight binding at 4 °C. Next day, beads were washed three times with PBS plus 0.2% Triton X-100, and samples were eluted in 5× sample buffer. Samples were subjected to traditional Western blotting and probed for CFTR using FLAG antibody.

Intestinal fluid secretion (in vivo) measurement or closed intestinal loop experiment

Adcy6$^{f/f}$ and *Adcy6*$^{\Delta/\Delta}$ mice were starved for 24 h before surgery. Mice were anesthetized under isofluorane with optimal O_2 and placed on a warm pad to maintain body temperature. A small abdominal incision was made to expose the distal region of small intestine. Intestinal loops (~2 cm) were exteriorized and isolated (two loops per mouse). The closed loops were then injected with 100 μl of PBS alone or PBS containing CTX (1 and 10 μg) or linaclotide (1 μg). The abdominal incision and skin incision were closed with surgical sutures, and the mice were allowed to recover. After 6 h, the mice were sacrificed by CO_2. Intestinal loops were removed, and loop fluid weight was measured to quantitate net fluid secretion.

Intestinal crypt isolation and quantitation of fluid secretion in enterospheres

Preparation of mouse intestinal crypt and quantitation were performed as described previously (19). For fluid secretion measurement with the high-content microscope (Lionheart^{TM} FX, Biotek), average organoid area was calculated pre- and post-forskolin treatment.

Isolation of tracheal epithelial cells and short circuit current (I_{sc}) measurements

The protocol for isolation of tracheal cells was followed as described previously (29). Mouse tracheal cells were polarized on Costar Transwell permeable supports (Cambridge, MA) (filter diameter, 12 mm). After 21 days of culturing, transwells were mounted in an Ussing chamber system (Physiologic Instruments) maintained at 37 °C (30). Epithelial cells were bathed in Ringer's solution (basolateral side: 140 mM NaCl, 5 mM KCl, 0.36 mM K_2HPO_4, 0.44 mM KH_2PO_4, 1.3 mM $CaCl_2$, 0.5 mM $MgCl_2$, 4.2 mM $NaHCO_3$, 10 mM HEPES, 10 mM glucose, pH 7.2, [Cl^-] = 149 mM) and low-Cl^- Ringer's solution (apical side: 133.3 mM sodium gluconate, 2.5 mM NaCl, 0.36 mM

K_2HPO_4, 0.44 mM KH_2PO_4, 5.7 mM $CaCl_2$, 0.5 mM $MgCl_2$, 4.2 mM $NaHCO_3$, 10 mM HEPES, 10 mM mannitol, pH 7.2, $[Cl^-]$ = 14.8). Cells were treated first with amiloride (50 μM), and, after current stabilization, CFTR was activated by adding 10 μM forskolin on the apical side. CFTRinh-172 (20–50 μM) was added to the apical side to verify CFTR dependence of the currents. Calcium-dependent currents were activated in the presence of ATP (100 μM) added to the apical side at the end of the experiment.

Immunofluorescence and proximity ligation assay

Paraffin-embedded mouse ileum segments were stained for CFTR and AC6 proteins as follows. Slides were deparaffinized in xylene three times, 5 min each, followed by dehydration with ethanol. Antigen retrieval was performed with Borg DeCloaker RTU (Biocare Medical, Concord, CA) in a pressure cooker for 5–10 min. Slides were cooled for 5 min, and tissues were permeabilized with 0.2% Triton X-100 in PBS for 10 min. Tissues were then blocked in 2.5% horse serum overnight. Slides were rinsed with 1× PBS and incubated with rabbit polyclonal AC5/6 (1:25 dilution) and mouse monoclonal CF3 (1:25 dilution) antibodies at 4 °C overnight. Human organoids embedded in Matrigel were fixed with 4% formaldehyde and permeabilized with 0.2% Triton X-100 in PBS for 30 min. Samples were incubated with rabbit polyclonal AC5/6 (1:25 dilution) and mouse CFTR antibody R1104 (1:50 dilution) for 24 h at 4 °C.

For the proximity ligation assay, anti-rabbit (plus) and anti-mouse (minus) Duo link In Situ PLA probes (MilliporeSigma) were added to the samples incubated with anti-AC5/6 and anti-CFTR antibodies as mentioned above. The next steps of PLA assay were completed as described in the manufacturer's protocol. Slides were examined using a confocal microscope (Olympus FV1200).

FRET microscopy and data analysis

For direct sensitized emission FRET, HT29CL19A cells were transiently transfected with pAMCyan-AC6 and pEYFP-CFTR singly or in combination using Lipofectamine 3000. Single transfected cells were used to acquire cyan– or yellow fluorescent protein–only images for bleedthrough calculations. The corrected FRET (FRETc) was normalized with donor cyan fluorescent protein intensity (FRETc/cyan fluorescent protein), yielding the normalized corrected FRET (N-FRETc), and the intensity of N-FRETc images was presented in pseudocolor and monochrome mode, stretched between the low and high normalization values, according to an intensity-to-color mapped lookup table. All calculations were performed with the Channel Math and FRET modules of SlideBook software version 4.2 (Intelligent Imaging Innovations, Denver, CO).

Measurement of whole-cell cAMP and cGMP

Adcy6$^{f/f}$ and *Adcy6*$^{\Delta/\Delta}$ enterospheres were treated with FSK (10 μM, 1 h), CTX (100 ng, 24 h) and linaclotide (500 nM, 24 h) at 37 °C in the presence of isobutylmethylxanthine. Enterospheres were lysed in 0.1 N HCl, 0.2% Triton X-100 and centrifuged at 800 × *g*, and the supernatant was collected and used for cAMP- or cGMP-specific ELISA following the manufacturer's protocol (Enzo Life Science, Farmingdale, NY).

Author contributions—K. A. and A. P. N. conceived and supervised the project. A. T., Y. R., and K. A. designed and performed experiments and together wrote the manuscript. A. P. N. edited the draft manuscript. K. M. assisted in the human enterosphere experiment.

Acknowledgment—We are grateful to Dr. Gail Pyne-Geithman for editing the manuscript.

References

1. Finkelstein, R. A. (1996) Cholera, *Vibrio cholerae* O1 and O139, and other pathogenic vibrios. In *Medical Microbiology* (Baron, S., ed) 4th Ed, Chapter 24, University of Texas Medical Branch at Galveston, Galveston, TX
2. Vanden Broeck, D., Horvath, C., and De Wolf, M. J. (2007) *Vibrio cholerae*: cholera toxin. *Int. J. Biochem. Cell Biol.* **39,** 1771–1775 CrossRef Medline
3. Li, C., Dandridge, K. S., Di, A., Marrs, K. L., Harris, E. L., Roy, K., Jackson, J. S., Makarova, N. V., Fujiwara, Y., Farrar, P. L., Nelson, D. J., Tigyi, G. J., and Naren, A. P. (2005) Lysophosphatidic acid inhibits cholera toxin-induced secretory diarrhea through CFTR-dependent protein interactions. *J. Exp. Med.* **202,** 975–986 CrossRef Medline
4. Field, M. (2003) Intestinal ion transport and the pathophysiology of diarrhea. *J. Clin. Invest.* **111,** 931–943 CrossRef Medline
5. Cutting, G. R. (2015) Cystic fibrosis genetics: from molecular understanding to clinical application. *Nat. Rev. Genet.* **16,** 45–56 CrossRef Medline
6. Gabriel, S. E., Brigman, K. N., Koller, B. H., Boucher, R. C., and Stutts, M. J. (1994) Cystic fibrosis heterozygote resistance to cholera toxin in the cystic fibrosis mouse model. *Science* **266,** 107–109 CrossRef Medline
7. Li, C., and Naren, A. P. (2005) Macromolecular complexes of cystic fibrosis transmembrane conductance regulator and its interacting partners. *Pharmacol. Ther.* **108,** 208–223 CrossRef Medline
8. Guggino, W. B., and Stanton, B. A. (2006) New insights into cystic fibrosis: molecular switches that regulate CFTR. *Nat. Rev. Mol. Cell Biol.* **7,** 426–436 CrossRef Medline
9. Arora, K., Moon, C., Zhang, W., Yarlagadda, S., Penmatsa, H., Ren, A., Sinha, C., and Naren, A. P. (2014) Stabilizing rescued surface-localized deltaf508 CFTR by potentiation of its interaction with Na^+/H^+ exchanger regulatory factor 1. *Biochemistry* **53,** 4169–4179 CrossRef Medline
10. Cheng, J., Wang, H., and Guggino, W. B. (2004) Modulation of mature cystic fibrosis transmembrane regulator protein by the PDZ domain protein CAL. *J. Biol. Chem.* **279,** 1892–1898 CrossRef Medline
11. Hanoune, J., and Defer, N. (2001) Regulation and role of adenylyl cyclase isoforms. *Annu. Rev. Pharmacol. Toxicol.* **41,** 145–174 CrossRef Medline
12. Sabbatini, M. E., D'Alecy, L., Lentz, S. I., Tang, T., and Williams, J. A. (2013) Adenylyl cyclase 6 mediates the action of cyclic AMP-dependent secretagogues in mouse pancreatic exocrine cells via protein kinase A pathway activation. *J. Physiol.* **591,** 3693–3707 CrossRef Medline
13. Ma, J., Zhao, J., Drumm, M. L., Xie, J., and Davis, P. B. (1997) Function of the R domain in the cystic fibrosis transmembrane conductance regulator chloride channel. *J. Biol. Chem.* **272,** 28133–28141 CrossRef Medline
14. Söderberg, O., Gullberg, M., Jarvius, M., Ridderstråle, K., Leuchowius, K. J., Jarvius, J., Wester, K., Hydbring, P., Bahram, F., Larsson, L. G., and Landegren, U. (2006) Direct observation of individual endogenous protein complexes *in situ* by proximity ligation. *Nat. Methods* **3,** 995–1000 CrossRef Medline
15. Chey, W. D., Lembo, A. J., Lavins, B. J., Shiff, S. J., Kurtz, C. B., Currie, M. G., MacDougall, J. E., Jia, X. D., Shao, J. Z., Fitch, D. A., Baird, M. J., Schneier, H. A., and Johnston, J. M. (2012) Linaclotide for irritable bowel syndrome with constipation: a 26-week, randomized, double-blind, placebo-controlled trial to evaluate efficacy and safety. *Am. J. Gastroenterol.* **107,** 1702–1712 CrossRef Medline
16. Ma, T., Thiagarajah, J. R., Yang, H., Sonawane, N. D., Folli, C., Galietta, L. J., and Verkman, A. S. (2002) Thiazolidinone CFTR inhibitor identified by high-throughput screening blocks cholera toxin-induced intestinal fluid secretion. *J. Clin. Invest.* **110,** 1651–1658 CrossRef Medline
17. Arora, K., Huang, Y., Mun, K., Yarlagadda, S., Sundaram, N., Kessler, M. M., Hannig, G., Kurtz, C. B., Silos-Santiago, I., Helmrath, M., Palermo,

J. J., Clancy, J. P., Steinbrecher, K. A., and Naren, A. P. (2017) Guanylate cyclase 2C agonism corrects CFTR mutants. *JCI Insight* **2,** 93686 Medline

18. Sato, T., and Clevers, H. (2013) Growing self-organizing mini-guts from a single intestinal stem cell: mechanism and applications. *Science* **340,** 1190–1194 CrossRef Medline
19. Moon, C., Zhang, W., Ren, A., Arora, K., Sinha, C., Yarlagadda, S., Woodrooffe, K., Schuetz, J. D., Valasani, K. R., de Jonge, H. R., Shanmukhappa, S. K., Shata, M. T., Buddington, R. K., Parthasarathi, K., and Naren, A. P. (2015) Compartmentalized accumulation of cAMP near complexes of multidrug resistance protein 4 (MRP4) and cystic fibrosis transmembrane conductance regulator (CFTR) contributes to drug-induced diarrhea. *J. Biol. Chem.* **290,** 11246–11257 CrossRef Medline
20. Dekkers, J. F., Wiegerinck, C. L., de Jonge, H. R., Bronsveld, I., Janssens, H. M., de Winter-de Groot, K. M., Brandsma, A. M., de Jong, N. W., Bijvelds, M. J., Scholte, B. J., Nieuwenhuis, E. E., van den Brink, S., Clevers, H., van der Ent, C. K., Middendorp, S., and Beekman, J. M. (2013) A functional CFTR assay using primary cystic fibrosis intestinal organoids. *Nat. Med.* **19,** 939–945 CrossRef Medline
21. Torres, V. E., and Harris, P. C. (2014) Strategies targeting cAMP signaling in the treatment of polycystic kidney disease. *J. Am. Soc. Nephrol.* **25,** 18–32 CrossRef Medline
22. Melis, N., Tauc, M., Cougnon, M., Bendahhou, S., Giuliano, S., Rubera, I., and Duranton, C. (2014) Revisiting CFTR inhibition: a comparative study of CFTRinh-172 and GlyH-101 inhibitors. *Br. J. Pharmacol.* **171,** 3716–3727 CrossRef Medline
23. Arora, K., Sinha, C., Zhang, W., Ren, A., Moon, C. S., Yarlagadda, S., and Naren, A. P. (2013) Compartmentalization of cyclic nucleotide signaling: a question of when, where, and why? *Pflugers Arch.* **465,** 1397–1407 CrossRef Medline
24. Cheepala, S., Hulot, J. S., Morgan, J. A., Sassi, Y., Zhang, W., Naren, A. P., and Schuetz, J. D. (2013) Cyclic nucleotide compartmentalization: contributions of phosphodiesterases and ATP-binding cassette transporters. *Annu. Rev. Pharmacol. Toxicol.* **53,** 231–253 CrossRef Medline
25. Dessauer, C. W., Watts, V. J., Ostrom, R. S., Conti, M., Dove, S., and Seifert, R. (2017) International Union of Basic and Clinical Pharmacology. CI. Structures and small molecule modulators of mammalian adenylyl cyclases. *Pharmacol. Rev.* **69,** 93–139 CrossRef Medline
26. Foulke-Abel, J., In, J., Yin, J., Zachos, N. C., Kovbasnjuk, O., Estes, M. K., de Jonge, H., and Donowitz, M. (2016) Human enteroids as a model of upper small intestinal ion transport physiology and pathophysiology. *Gastroenterology* **150,** 638–649.e8 CrossRef Medline
27. Pasyk, S., Molinski, S., Ahmadi, S., Ramjeesingh, M., Huan, L. J., Chin, S., Du, K., Yeger, H., Taylor, P., Moran, M. F., and Bear, C. E. (2015) The major cystic fibrosis causing mutation exhibits defective propensity for phosphorylation. *Proteomics* **15,** 447–461 CrossRef Medline
28. Bozoky, Z., Ahmadi, S., Milman, T., Kim, T. H., Du, K., Di Paola, M., Pasyk, S., Pekhletski, R., Keller, J. P., Bear, C. E., and Forman-Kay, J. D. (2017) Synergy of cAMP and calcium signaling pathways in CFTR regulation. *Proc. Natl. Acad. Sci. U.S.A.* **114,** E2086–E2095 CrossRef Medline
29. You, Y., Richer, E. J., Huang, T., and Brody, S. L. (2002) Growth and differentiation of mouse tracheal epithelial cells: selection of a proliferative population. *Am. J. Physiol. Lung Cell Mol. Physiol.* **283,** L1315–L1321 CrossRef Medline
30. Li, C., Krishnamurthy, P. C., Penmatsa, H., Marrs, K. L., Wang, X. Q., Zaccolo, M., Jalink, K., Li, M., Nelson, D. J., Schuetz, J. D., and Naren, A. P. (2007) Spatiotemporal coupling of cAMP transporter to CFTR chloride channel function in the gut epithelia. *Cell* **131,** 940–951 CrossRef Medline